First-Principles Study of Chemisorption of Oxygen and Aziridine on Graphitic Nanostructures

Alex Kutana and Konstantinos P. Giapis*

Division of Chemistry and Chemical Engineering, California Institute of Technology, Pasadena, California 91125

Received: May 15, 2009

Using ab initio plane wave pseudopotential calculations, we study the energetics and structure of adsorbed linear arrays of oxygen and aziridine on carbon nanotubes, graphitic ribbons, and graphene sheets. Chemisorption of arrays of O or NH causes splitting of the CC bond and local deformation of the graphitic structures. The (3,3) nanotube cross section assumes a teardrop-like shape, while graphene sheets warp into a new local geometry around the chemisorbed molecules. The interior of a (3,3) nanotube is less prone to oxidation than the exterior because of steric effects. A zigzag (6,0) nanotube is less reactive and thus chemically more stable than an armchair (3,3) nanotube. The results suggest a partial explanation for the experimentally observed selective etching of metallic carbon nanotubes.

I. Introduction

The reactive modification of carbon nanotubes and other graphitic materials is of fundamental and practical interest.[1−3] Covalent bonding of nanotubes with other atoms or molecules is a required step for functionalizing the nanotubes with biomaterials and for integrating them into nanoelectronics.[4] The electronic properties of carbon nanotubes are extremely sensitive to changes in their chemical environment.[5] Specifically, attaching atoms or molecules to a nanotube wall may lead to materials with new electronic properties. This effect was found to be considerable in ab initio calculations of atomic[6,7] and molecular[6−8] oxygen adsorption on the outer surfaces of zigzag and armchair nanotubes. Elsewhere, even small amounts of adsorbed aryl[9] were predicted to influence dramatically the nanotube conductivity. Adsorption and bonding of isolated atoms or radicals on nanotube walls may be accompanied by structural changes. Most of the published work thus far has dealt with situations where structural changes in the nanotubes are typically small.

In this paper, we consider large structural changes in nanotubes, ensuing from functionalization with rows of adsorbed atoms or radicals, in particular the "unzipping" of nanotubes caused by chemisorption. Oxygen can form epoxides by binding above the CC bonds in graphene-based structures. The high angular strain in the epoxide rings, when arranged in a row, may cause the CC bonds to unravel in concerted fashion, leading to the unzipping of the graphitic material.[10] When fully understood, the reactive unzipping process may be useful in manipulating the shape and functionality of graphene-based materials. For instance, oxidative unzipping of nanotubes may lead to the formation of nanoribbons at precise locations on wafers, thus enabling nanoelectronics applications. Epoxidation is not the only way to unzip carbon nanotubes. For example, the experimentally proven external functionalization of nanotubes with aziridothymidine using photodissociation of the azide group,[11] suggests that nitridization may offer an alternative pathway with possible advantages over epoxidation.

We present here results from a first principles theoretical study of the chemical interaction of atomic oxygen and aziridine with nanoscale graphitic materials of various curvature, size, and chirality. More specifically, we discuss the energetics of and the structural changes resulting from the chemisorption of rows of O and NH on the inner and outer walls of a (3,3) armchair carbon nanotube, on graphitic ribbons and graphene sheets, and on a (6,0) zigzag nanotube. Adsorption energies, equilibrium C−C bond lengths, and C−O−C (or C−NH−C) angles are calculated for multiple configurations.

II. Method

All calculations were carried out using the ABINIT electronic structure program.[12] We employed density functional theory (DFT) with the Perdew−Burke−Ernzerhof (PBE) exchange-correlation GGA functional.[13] A plane wave basis set with a cutoff energy of 35 hartree (1 hartree = 27.2114 eV) was used to represent the wave functions during geometry optimizations. The calculations for the final equilibrium minimum-energy structures were carried out using plane waves with a higher energy cutoff of 60 hartree. The norm-conserving pseudopotentials for atoms were generated with the fhi98pp program,[14] following the procedure of Troullier and Martins.[15] The Brillouin zone sampling was carried out on 16 × 16 × 1 (2D structures) and 16 × 1 × 1 (1D structures) Monkhorst-Pack grids,[16] while energies and eigenstates of isolated systems were evaluated at the Γ point only.

Spin up and spin down polarizations were accounted for in calculations of isolated atoms and molecules, as well as extended structures. Spin polarization directions were chosen normal to the axis of the tube, or normal to the plane of the graphitic ribbon or sheet for ferromagnetic and antiferromagnetic states in periodic structures. The degree of magnetization was evaluated using the relative magnetization density ζ, defined as

$$\zeta = (n_\uparrow - n_\downarrow)/(n_\uparrow + n_\downarrow)$$

where $n_\uparrow$ and $n_\downarrow$ are electronic densities for spin up and spin down polarizations, correspondingly. Significant spatial separations of spin up and spin down densities were found for antiferromagnetic states in pristine and decorated graphitic

* Corresponding author. E-mail: giapis@cheme.caltech.edu.

10.1021/jp904555n CCC: $40.75
Published on Web 06/22/2009

ribbons, whereas other extended structures turned out to be spin-unpolarized in their ground states.

Minimum energy geometries were obtained using the Broyden optimization algorithm.[17] The minimization procedure was considered converged when the maximum component of the force acting on any atom was smaller than 2.6×10^{-3} eV/Å.

III. Results and Discussion

The first series of calculations address the interaction of pristine nanotubes with oxygen. The minimum energy structure of a (3,3) nanotube decorated with atomic oxygen on the outside is shown in Figure 1a, whereas the structure with oxygen inside is shown in Figure 1b. Both structures are spin unpolarized, the maximum value of the relative magnetization density ζ being $\zeta = 2.3 \times 10^{-3}$.

The starting configuration for the structure in Figure 1a was an unperturbed (3,3) nanotube with an O atom on the outer wall. Each (n,n) nanotube has two types of symmetry nonequivalent CC bonds: the transverse bonds that are perpendicular to the tube axis and those that are slanted at approximately 30° with respect to the axis. The initial position of the oxygen atom was above the transverse bond at a radial distance 1.1 Å from the bond center. The supercell with 12 carbon and 1 oxygen atoms is repeated periodically along the axis, so that oxygen atoms and corresponding transverse CC bonds below them form a row. The dimensions of the supercell in the lateral directions were 15.3 Å, ensuring that the interactions between neighboring images are negligible.

The oxygen-substrate interaction leads to the splitting of the transverse CC bonds, and also changes the nanotube cross section from circular to teardrop like, as shown on the inset of Figure 1a. This deformation of the nanotube shape does not contribute significantly to the decrease of the total energy of the system. Instead, the main contribution to the adsorption energy comes from the local bonding rearrangement around the O atom. The adsorption energy was calculated according to the formula

$$E_{\mathrm{ads}}^{\mathrm{SWNT}} = E[\mathrm{SWNT} + \mathrm{O}] - (E[\mathrm{SWNT}] + E[\mathrm{O}]) \quad (1)$$

where E[SWNT + O] is the energy of the nanotube with adsorbed oxygen, E[SWNT] is the energy of the pristine nanotube, and E[O] is the energy of the oxygen atom in the ^3P ground state. The values of the energy minima obtained using eq 1 are given in Table 1.

In addition, E_{ads} was calculated as a function of the transverse CC bond length, as shown in Figure 2a. For each point, the distance between the two C atoms was kept fixed, while all other atoms were allowed to move during the minimum energy search. The transition from the initial configuration to the minimum energy state has no activation barrier, indicating that the oxygen adsorption and the splitting of transverse CC bonds would occur spontaneously at any temperature.

There is a significant reduction in energy (−3.68 eV) at the first point, where the CC bond distance equals that of the unperturbed bond (1.43 Å). The nanotube cross section deviates significantly from circular at this point, and assumes the teardrop-like shape shown in the inset of Figure 1a. This shape is maintained at each point along the descent to a minimum in Figure 2a. It is interesting to estimate the contribution of the overall shape change to the initial stabilization energy of −3.68 eV. This amount of energy can be calculated by considering the structure with the same local COC geometry, but a circular cross section. It turns out that the energy of such structure is −3.26 eV, so that the contribution from the nonlocal deformation of the cross section to the stabilization energy is only −0.42 eV.

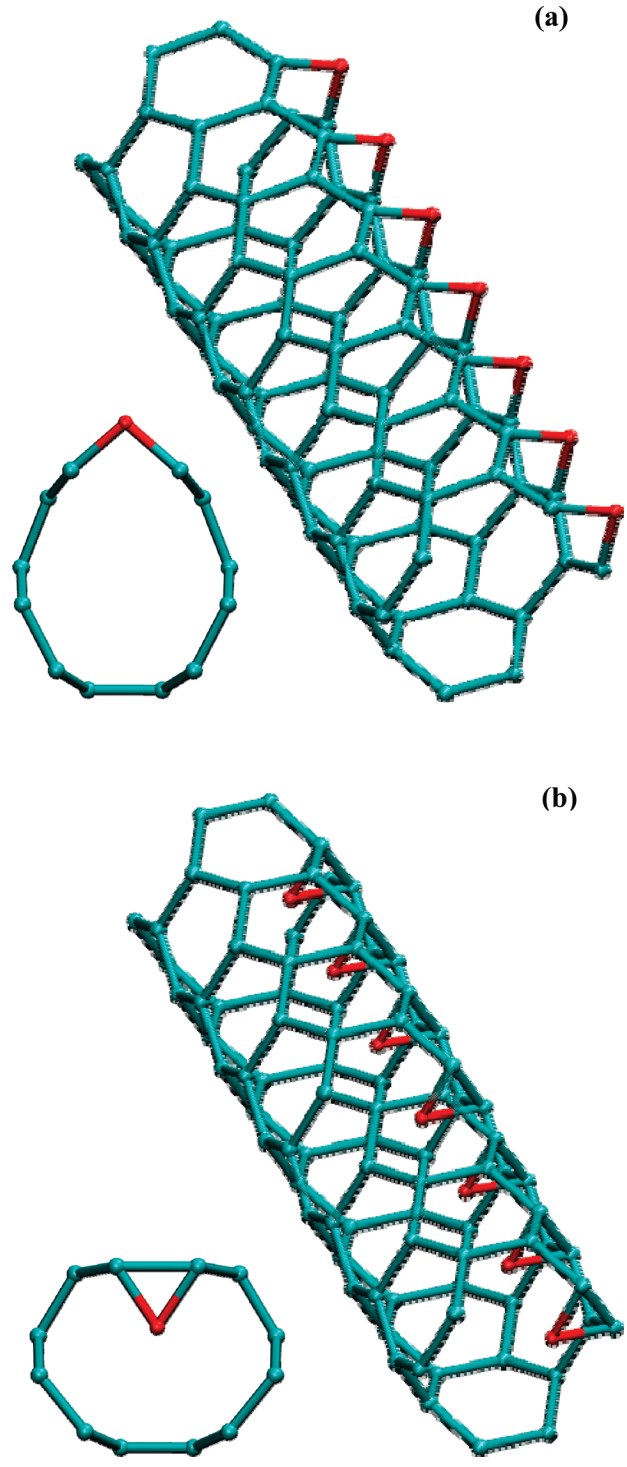

Figure 1. Minimum energy structures of a (3,3) nanotube decorated with oxygen, as predicted by ab initio simulations for (a) external O attachment, (b) internal O attachment. Bonds and atoms within the supercell are opaque, while those of their periodic images are transparent. The insets show the respective cross sections of the nanotube. All illustrations of molecules have been prepared using the VMD software package.[22]

Now consider the interaction of an oxygen atom with the inner wall of the (3,3) nanotube. The structure shown in Figure

TABLE 1: Geometric Parameters, Adsorption Energies, of Atomic Oxygen on Carbon Nanotubes, Graphitic Ribbons, and Graphene

	E_{ads}, eV	C−C bond distance, Å	C−O−C angle, deg
(3,3) SWNT outer wall	−5.06	2.12	98.1
(3,3) SWNT inner wall	−0.35	1.57	67.5
(6,0) SWNT outer wall	−3.68	1.48	61.7
(3,3) graphitic ribbon	−3.40	2.47	131.6
graphene sheet	−3.23	2.53	139.8

1b was obtained by minimizing the total energy of a pristine (3,3) nanotube with an O atom positioned inside at a radial distance 1.1 Å from the center of the transverse CC bond. After the minimization, the epoxide rings at the oxygen adsorption site are still effectively closed at CC distance of 1.57 Å. In contrast with the external oxidation, where the system is stabilized by −5.06 eV, the energy minimum of only −0.34 eV is rather shallow. As the obtained adsorption energy is so small-comparable in magnitude to van der Waals interaction energy-its evaluation should be approached with care, due to the inability of GGA exchange-correlation functionals to treat van der Waals interactions. Thus, the relative error for the adsorption energy on the inner wall will be larger than the error in all other cases of higher adsorption energies.

The quantitative and qualitative differences between oxygen chemisorption over transverse bonds at internal and external sites in a (3,3) tube can be understood by comparing the energy dependence on CC bond length. As inferred from Figure 2b, there exists an energy barrier that prevents the epoxide rings from opening when the O atom is placed inside the nanotube. In contrast, there is no such barrier for O atoms positioned on the outside of the tube. Thus, the transverse CC bond in the

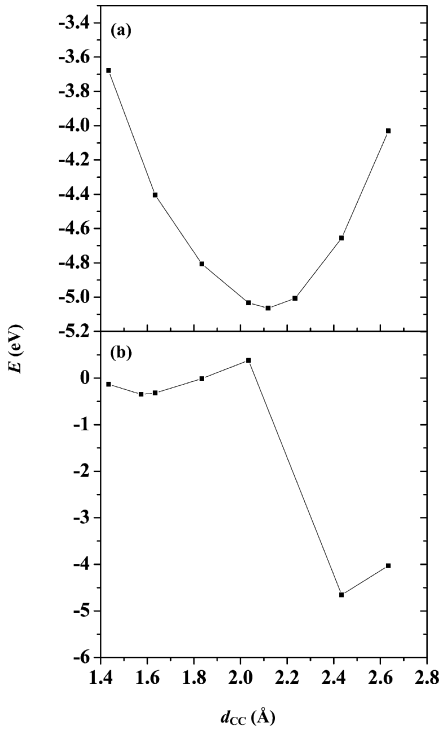

Figure 2. Energy of adsorption of oxygen over the transverse CC bond in a (3,3) SWNT as a function of the CC bond length for (a) external O attachment and (b) internal O attachment. (b) The precipitous drop in energy between 2.0 and 2.4 Å corresponds to the switching of oxygen atoms from the inside to outside positions. The points are connected with lines to assist interpretation.

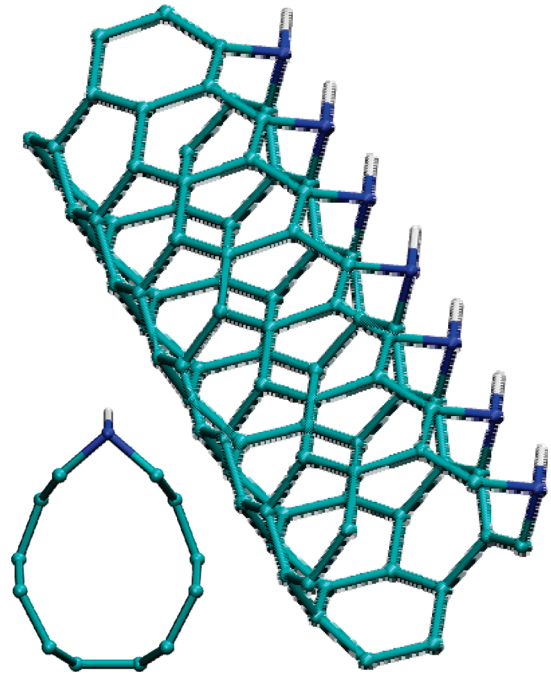

Figure 3. Minimum energy structure of a (3,3) nanotube decorated with aziridine, as predicted by ab initio simulations. Bonds and atoms within the supercell are opaque, while their periodic images are transparent. The inset shows the cross section of the nanotube.

(3,3) tube is less reactive toward oxygen in the local environment created by concave nanotube walls. When the C−O−C bond angle can be made large enough, the structure becomes inverted, and the O atom appears on the outside. The precipitous drop in energy from a bond length of 2.0 to 2.4 Å corresponds to the flipping of oxygen atoms from inside to outside positions, recovering the configuration of Figure 1a.

The functionalization of the (3,3) nanotube with the NH (aziridine) group is in many respects analogous to the case of the O atom considered above. In complete correspondence with the O case, splitting of the CC bond occurs during the attachment of the NH group to the nanotube outer wall. Figure 3 shows the resulting structure with the split CC bonds, and the characteristic teardrop-like cross section (see inset). The functional group assumes a trigonal pyramidal shape, with the N atom at the apex of the pyramid, and NH, NC bonds forming its edges. The energy of adsorption, E_{ads}, was calculated using the formula

$$E_{ads}^{SWNT} = E[\text{SWNT} + \text{NH}] - (E[\text{SWNT}] + E[\text{NH}]) \quad (2)$$

Here, E[SWNT + NH] is the energy of the nanotube with the attached aziridine groups, and E[NH] is the energy of the NH molecule in the $^3\Sigma$ ground state. The calculated energies and geometric parameters are given in Table 2.

The energy for the adsorption of the NH group as a function of the length of the CC bond is shown in Figure 4, and is similar to the O case. The stabilization energy at the equilibrium CC bond length is −3.21 eV. The system proceeds from the initial state, at equilibrium CC bond length, to a global energy minimum without a barrier, indicating a spontaneous reaction.

The internal functionalization with NH is distinct from the O case, in that there is no energy barrier preventing the complete opening of CC bonds. Hence, the metastable state characterized

TABLE 2: Geometric Parameters and Adsorption Energies of Aziridine on Carbon Nanotubes, Graphitic Ribbons, and Graphene

	E_{ads}, eV	C−C bond distance, Å	C−N−C angle, deg
(3,3) SWNT outer wall	−4.11	2.20	98.2
(6,0) SWNT outer wall	−1.69	1.54	66.5
(3,3) graphitic ribbon	−2.30	2.33	107.9
graphene sheet	−1.44	2.48	124.1

by the weak inner adsorption over the transverse bonds does not exist for aziridine. The minimization procedure leads to the final state identical to the external functionalization, with aziridine groups flipping to the outside position by inverting their CNC angles. The ground state is spin unpolarized, with the maximum ζ value of $\zeta_{max} = 7.5 \times 10^{-4}$.

Since the curvature of the graphene sheet affects the geometry and energetics of the adsorption, it would be interesting to consider the oxidation of structures with zero curvature, such as graphitic ribbons. An (n,n) ribbon is obtained by opening an (n,n) nanotube along the transverse bonds and terminating unsaturated bonds with hydrogen atoms. Both pristine and hydrogen-terminated graphene ribbons are known to be antiferromagnetic in their ground state,[18,19] with the spin densities of opposite polarization localized at the edges. Our calculations yield an antiferromagnetic ground state with $\zeta_{max} = 0.25$, which is 0.083 eV below the unpolarized state for a (3,3) hydrogen-terminated ribbon.

The adsorption energies were calculated for (3,3) ribbons using formulas similar to eqs 1 and 2, modified appropriately for the energies of pristine and decorated ribbons. Figure 5 presents the longitudinal views of a (3,3) ribbon decorated with O atoms or NH groups. As a result of the interaction, the transverse CC bonds are split, just as in the previous calculations for nanotubes. The row of oxygen atoms divides the ribbon into two nearly planar segments, as shown in Figure 5a, giving it an inverted open V-shape. In the absence of the cylindrical geometry constraints pertinent to nanotubes, the adsorbed oxygen imposes the biplanar geometry. A similar shape, with a smaller interplanar angle is obtained for the ribbon decorated with NH, as seen in Figure 5b. Considering magnetic states in these structures, calculations suggest that the adsorption of oxygen or aziridine does not appreciably affect the antiferromagnetism of the (3,3) ribbon. In case of the O adsorption, the ground state is antiferromagnetic with $\zeta_{max} = 0.23$, and is 0.078 eV lower than the unpolarized state. For the NH adsorption,

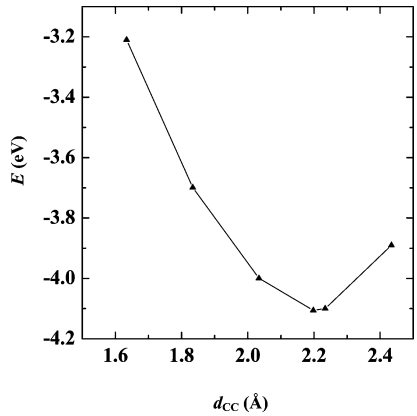

Figure 4. Energy of adsorption of aziridine over the transverse CC bond in a (3,3) SWNT as a function of the CC bond length. The points are connected with lines to assist interpretation.

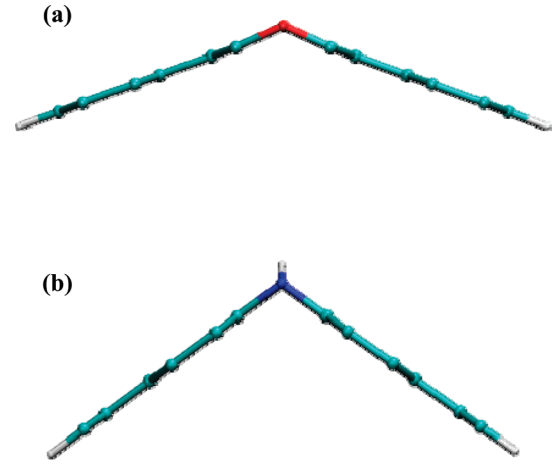

Figure 5. Longitudinal views of a (3,3) hydrogen-terminated graphitic ribbon decorated with (a) oxygen, and (b) aziridine.

the ground state is also antiferromagnetic with $\zeta_{max} = 0.23$, and is 0.073 eV lower than the unpolarized state.

In all cases of decorating CC bonds with O and NH considered above, the local environment around the adsorbate changed drastically during the CC bond splitting. As the adsorbate imposes the new local geometry, a long-range distortion of the graphitic structure may occur. For instance, a row of oxygen atoms adsorbed on a graphene sheet creates a local environment in its vicinity similar to that in a (3,3) tube in Figure 1a. Adding another row of adsorbed atoms next to it would create an identical local environment that would have to be reconciled with the first one through the deformations of the graphene sheet. An example of such interaction between the rows is given in Figure 6a, where the structure of a graphene sheet with oxygen rows separated by four elementary cells is shown. The interaction results in the warping of the segment between the rows. The warping also occurs as a result of the adsorption of the rows of aziridine groups, as shown in Figure 6b. It is noted that such a warping deformation is critical for bond splitting. If the energy required for warping is too high (e.g., when rows of oxygen atoms are too close to each other), an energy barrier for bond splitting appears.

In a highly strained epoxide ring, the bonding between the two C atoms is almost balanced out by the ring strain. Consequently, any additional perturbations of the ring such as a change in coordination or steric hindrance may either shift the balance toward ring-opening or make it more stable. For instance, when the deformations of graphene structures considered above cannot occur because of steric effects, the epoxide rings will remain closed. In an (n,0) single-walled nanotube, there are n longitudinal CC bonds parallel to the tube axis. Oxidative splitting of these bonds requires longitudinal warping of the walls, which is energetically not favorable. Without bond splitting, the resulting geometry differs little from that of the original (6,0) tube (see Figure 7). In this case, the equilibrium CC bond distance of 1.48 Å is close to that of the pristine tube. However, the high adsorption energy of −3.68 eV indicates that there exists strong chemical interaction between the adsorbate and substrate.

The structure of the graphitic material being modified affects not only the final geometry, but also the chemisorption energy. The chemisorption energies resulting in CC bond splitting and permanent changes in the structure of the nanotube are larger than the adsorption energies when neither splitting of CC bonds nor structural changes occur. Comparing the results for (3,3)

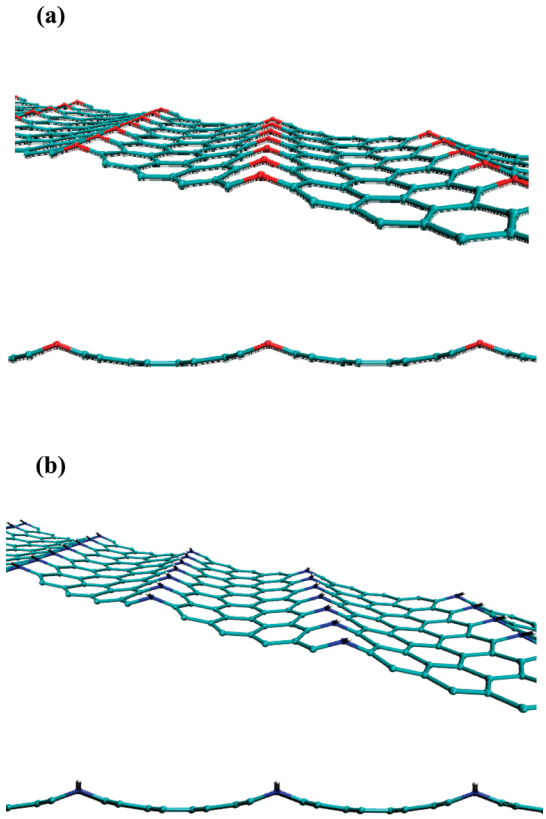

Figure 6. Minimum energy structure of graphene with (a) rows of oxygen atoms, and (b) rows of NH groups, adsorbed over CC bonds and separated by 4 elementary cells of graphene.

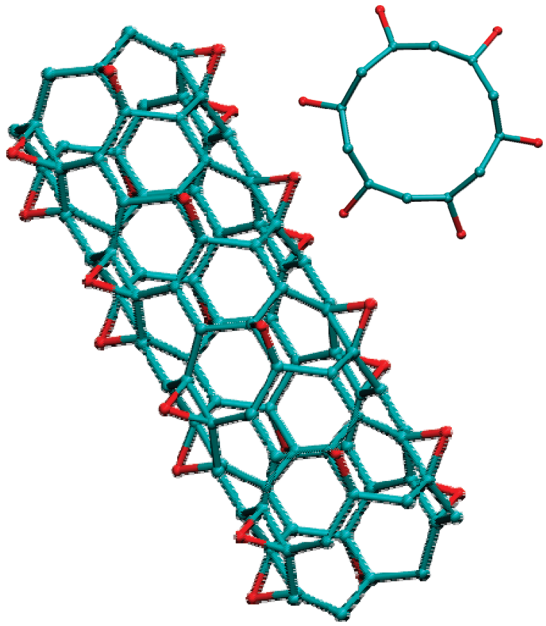

Figure 7. Minimum energy structure of a (6,0) nanotube with its longitudinal bonds decorated with oxygen.

and (6,0) nanotubes, it is clear that permanent structural changes occur in the transverse bonds of armchair nanotubes, while the longitudinal bonds of zigzag tubes are not affected. If this result can be generalized for larger nanotubes, it may explain the experimental observation of the preferential etching of metallic nanotubes over semiconducting ones.[20] However, this explanation would apply only to (n,n) metallic nanotubes, and not all (n,m) nanotubes for which a metallicity condition $2n + m = 3q$ is satisfied.[21] For a full explanation of the observed preferential etching, an exhaustive study of adsorption on all kinds of chiral nanotubes must be undertaken.

A comparison of Tables 1 and 2 suggests that the adsorption energies are generally greater for O than NH. Despite its weaker bonding, NH chemisorption to graphitic structures could enable their functionalization through the covalent attachment of long graft molecules. Our study provides an illustration of the energetics and geometry of the adsorption of aziridine.

IV. Conclusions

We have performed first principles calculations to study the reactivity of oxygen and aziridine on periodic graphitic structures. In most structures (exterior of (3,3) armchair nanotubes and graphene sheets), the CC bonds are found to be reactive and prone to oxygen and aziridine attack. Significant deformations of the graphitic structures are observed during chemical binding of O and NH. The adsorption of oxygen on the inner wall of a (3,3) nanotube displays a shallow local energy minimum characterized by a nearly intact CC bond. Similarly, adsorption of O or NH on the outer wall of a (6,0) nanotube shows reduced reactivity in comparison to a (3,3) nanotube. These findings offer a partial explanation of the experimentally observed selective etching of metallic carbon nanotubes.

Acknowledgment. This material was based in part upon work supported by the National Science Foundation (CTS-0613981).

References and Notes

(1) Bianco, A.; Kostarelos, K.; Prato, M. Applications of carbon nanotubes in drug delivery. *Curr. Opin. Chem. Biol.* **2005**, *9* (6), 674–679.
(2) Wang, J. Carbon-nanotube based electrochemical biosensors: A review. *Electroanalysis* **2005**, *17* (1), 7–14.
(3) Sinha, N.; Ma, J. Z.; Yeow, J. T. W. Carbon nanotube-based sensors. *J. Nanosci. Nanotechnol.* **2006**, *6* (3), 573–590.
(4) Katz, E.; Willner, I. Biomolecule-functionalized carbon nanotubes: Applications in nanobioelectronics. *ChemPhysChem* **2004**, *5* (8), 1085–1104.
(5) Collins, P. G.; Bradley, K.; Ishigami, M.; Zettl, A. Extreme oxygen sensitivity of electronic properties of carbon nanotubes. *Science* **2000**, *287* (5459), 1801–1804.
(6) Dag, S.; Gulseren, O.; Yildirim, T.; Ciraci, S. Oxygenation of carbon nanotubes: Atomic structure, energetics, and electronic structure. *Phys. Rev. B* **2003**, *67* (16), 165424-1–165424-10.
(7) Liu, H. J.; Chan, C. T.; Liu, Z. Y.; Shi, J. Density functional study of oxygen adsorption on 4-angstrom carbon nanotubes. *Phys. Rev. B* **2005**, *72* (7), 075437-1–075437-6.
(8) Jhi, S. H.; Louie, S. G.; Cohen, M. L. Electronic properties of oxidized carbon nanotubes. *Phys. Rev. Lett.* **2000**, *85* (8), 1710–1713.
(9) Lee, Y. S.; Nardelli, M. B.; Marzari, N. Band structure and quantum conductance of nanostructures from maximally localized wannier functions: The case of functionalized carbon nanotubes. *Phys. Rev. Lett.* **2005**, *95* (7), 076804-1–076804-4.
(10) Li, J. L.; Kudin, K. N.; McAllister, M. J.; Prud'homme, R. K.; Aksay, I. A.; Car, R. Oxygen-driven unzipping of graphitic materials. *Phys. Rev. Lett.* **2006**, *96* (17), 176101-1–176101-4.
(11) Moghaddam, M. J.; Taylor, S.; Gao, M.; Huang, S. M.; Dai, L. M.; McCall, M. J. Highly efficient binding of DNA on the sidewalls and tips of carbon nanotubes using photochemistry. *Nano Lett.* **2004**, *4* (1), 89–93.
(12) Gonze, X.; Beuken, J. M.; Caracas, R.; Detraux, F.; Fuchs, M.; Rignanese, G. M.; Sindic, L.; Verstraete, M.; Zerah, G.; Jollet, F.; et al. First-principles computation of material properties: the ABINIT software project. *Comput. Mater. Sci.* **2002**, *25* (3), 478–492. www.abinit.org.
(13) Perdew, J. P.; Burke, K.; Ernzerhof, M. Generalized gradient approximation made simple. *Phys. Rev. Lett.* **1996**, *77* (18), 3865–3868.
(14) Fuchs, M.; Scheffler, M. Ab initio pseudopotentials for electronic structure calculations of poly-atomic systems using density-functional theory. *Comput. Phys. Commun.* **1999**, *119* (1), 67–98.
(15) Troullier, N.; Martins, J. L. Efficient Pseudopotentials for Plane-Wave Calculations. *Phys. Rev. B* **1991**, *43* (3), 1993–2006.
(16) Monkhorst, H. J.; Pack, J. D. Special Points for Brillouin-Zone Integrations. *Phys. Rev. B* **1976**, *13* (12), 5188–5192.
(17) Broyden, C. G. A Class of Methods for Solving Nonlinear Simultaneous Equations. *Math. Comput.* **1965**, *19* (92), 577–593.

(18) Fujita, M.; Wakabayashi, K.; Nakada, K.; Kusakabe, K. Peculiar localized state at zigzag graphite edge. *J. Phys. Soc. Jpn.* **1996**, *65* (7), 1920–1923.

(19) Son, Y. W.; Cohen, M. L.; Louie, S. G. Half-metallic graphene nanoribbons. *Nature* **2006**, *444* (7117), 347–349.

(20) Zhang, G. Y.; Qi, P. F.; Wang, X. R.; Lu, Y. R.; Li, X. L.; Tu, R.; Bangsaruntip, S.; Mann, D.; Zhang, L.; Dai, H. J. Selective etching of metallic carbon nanotubes by gas-phase reaction. *Science* **2006**, *314* (5801), 974–977.

(21) Saito, R.; Fujita, M.; Dresselhaus, G.; Dresselhaus, M. S. Electronic-Structure of Chiral Graphene Tubules. *Appl. Phys. Lett.* **1992**, *60* (18), 2204–2206.

(22) Humphrey, W.; Dalke, A.; Schulten, K. VMD: Visual molecular dynamics. *J. Mol. Graph.* **1996**, *14* (1), 33–38.

JP904555N